0026-895X/96/020244-09$3.00/0

MOLECULAR PHARMACOLOGY, 49:244–252 (1996).

Genesis of Discrete Higher Order DNA Fragments in Apoptotic Human Prostatic Carcinoma Cells

JAMES M. RUSNAK, THIERRY P. G. CALMELS, DALE G. HOYT, YUKIHIRO KONDO, JACK C. YALOWICH, and JOHN S. LAZO

Department of Pharmacology, University of Pittsburgh School of Medicine, Pittsburgh, Pennsylvania 15261, and the Experimental Therapeutics Program, Pittsburgh Cancer Institute, Pittsburgh, Pennsylvania 15261

Received June 16, 1995; Accepted October 16, 1995

SUMMARY

Higher order DNA fragmentation may be an essential signal in apoptosis. We found that etoposide (VP-16) induced apoptosis in human DU-145 prostatic carcinoma cells in a time- and concentration-dependent manner. Chromatin condensation was morphologically evident only when cells detached from the monolayer; untreated or VP-16-treated attached cells retained a normal morphology. We describe a radiolabeled *alu*-I sequence-based quantitative field inversion gel electrophoresis (QFIGE) method that permitted observation and quantification of discrete high molecular weight DNA fragments in detached (apoptotic) and attached (preapoptotic) DU-145 cells. The DNA fragments generated during the apoptotic death of these cells were ≥1 (mega-base pairs) mbp, 450–600 (kilo-base pairs) kbp, and 30–50 kbp; we observed that these DNA fragments increased 9 ± 2-, 8 ± 2-, and 25 ± 11-fold versus control, respectively, with a 24-hr exposure to 30 μM VP-16 in attached cell populations. In detached VP-16-treated cells, there was accrual of 30–50-kbp DNA fragments with a concomitant loss of the ≥1-mbp and 450–600-kbp fragments; internucleosomal DNA cleavage was never observed. This pattern of high molecular weight DNA fragmentation was inhibited by cycloheximide treatment and was common to other apoptotic agents, including melphalan and bleomycin. These findings suggest that the ≥1-mbp and 450–600-kbp DNA fragments are products of endonuclease activation and are not topoisomerase II/DNA interactions. Finally, the generation of the 30–50-kbp DNA fragments may mediate chromatin condensation, which characterizes apoptosis.

Apoptosis is a genetically regulated form of cell death; it occurs in tissues without the production of inflammation or secondary tissue damage. It is therefore considered the physiological form of cell death and is the homeostatic mechanism that offsets cellular proliferation. Cells undergo apoptosis after they receive appropriate cell death signals. These signals are either extracellular, as in apoptosis of T cell hybridomas after activation of the CD3 receptor complex (1), or intracellular, as in chemotherapeutic induction of apoptosis in tumor cells (2). Alternatively, cells undergo apoptosis after the withdrawal of cell survival signals, such as the regression of prostatic carcinomas after either surgical or pharmacological androgen ablation therapy (3).

Morphological changes during apoptosis include cell shrinkage and convolution of the plasma membrane, ultimately producing apoptotic bodies. It was the extensive nuclear changes, however, that were the paramount feature in the original description of apoptosis (4). Although considerable effort has been directed toward defining the biochemical basis for these morphological changes associated with apoptosis, no consensus has been achieved. Internucleosomal DNA fragmentation was once considered the hallmark of apoptosis and possibly causal in the morphological changes (5); this conclusion now seems unlikely with the demonstration of morphological apoptosis in the absence of internucleosomal DNA fragmentation in some cell types (6–14). Despite the universal presence of nuclear morphological changes, it has been suggested that the nucleus is nonessential for apoptosis (15, 16). Heralding this notion is the observation that some cytoplasmic changes associated with apoptosis are observed in enucleated cells after exposure to either an anti-APO-1/Fas antibody (15) or staurosporine (16). Genotoxic damage, however, is a powerful apoptotic stimulus, and it seems likely that the nucleus contains important mediators of the early events of apoptosis triggered by these agents. Indeed, some investigators have noted high molecular weight DNA fragments in apoptotic cells (6, 7, 17–21) and postulated that high molecular weight fragments could be an early critical event in apoptosis (7, 18).

This work was supported in part by National Institutes of Health Grant CA43917. J.M.R. was the recipient of a Pharmaceutical Research and Manufacturers of America Foundation, Inc., predoctoral fellowship.

ABBREVIATIONS: VP-16, etoposide; DMSO, dimethylsulfoxide; FIGE, field inversion gel electrophoresis; QFIGE, quantitative field inversion gel electrophoresis; CHX, cycloheximide; ISBE, *in situ* break extension; PBS, phosphate-buffered saline; SDS, sodium dodecyl sulfate; bp, base pair(s); HEPES, 4-(2-hydroxyethyl)-1-piperazineethanesulfonic acid.

The origins of higher order chromatin damage are unknown. Therefore, we examined DNA fragmentation in androgen-independent DU-145 cells and observed high molecular weight DNA breaks of ≥ 1 mbp, 450–600 kbp, and 30–50 kbp in attached cells that did not yet exhibit the morphological features of apoptosis. We believe that the attached cells having higher order DNA fragmentation represent a preapoptotic cell population. After cellular detachment, however, the ≥1-mbp and 450–600-kbp fragments were virtually undetectable, but there was an accrual of 30–50-kbp DNA fragments in cells that exhibited frank morphological evidence of apoptosis. Furthermore, as we found no indication of internucleosomal DNA cleavage in these apoptotic DU-145 cells, the generation of these 30–50-kbp DNA fragments may be essential for chromatin condensation and margination.

Finally, we tested the hypothesis that these ≥1-mbp and 450–600-kbp DNA fragments resulted from activation of an endonuclease rather than DNA double-strand breaks due to increased topoisomerase II/DNA cleavable religation complex formation. Importantly, topoisomerase II is a critical enzyme required for DNA replication, recombination, segregation of chromosomes, proper structure of DNA, and chromatin condensation and decondensation (22). Despite the lack of an identified role of topoisomerase II in mediating apoptosis, it is plausible that topoisomerase II participates in apoptosis by promoting chromatin condensation or facilitating endonuclease digestion of the genome. Moreover, VP-16-mediated stabilization of this religation complex has recently been reported to produce DNA fragments ranging from 600 kbp to >1 mbp (20, 21, 23). Our data support the hypothesis that these higher order DNA fragments were generated by endonuclease action and are not the result of topoisomerase II/DNA interactions.

Materials and Methods

Cell culture. Human DU-145 prostatic carcinoma cells (24) were obtained from American Type Culture Collection at passage 59 and were carried for no longer than 20 passages. The cells were grown in RPMI-1640 (GIBCO-BRL) containing 10% fetal bovine serum (HyClone), 100 units/ml penicillin G sodium, and 100 μg/ml streptomycin (GIBCO-BRL) at 37° under an atmosphere of 95% air/5% CO_2. To remove attached cells from the monolayer, we washed them three times with PBS and briefly treated them with 0.05% trypsin/2 mM EDTA at room temperature. After the addition of at least twice-volume of complete medium containing 10% fetal bovine serum, the cells were centrifuged at 1000 × *g* for 5 min. In some studies, cells already detached from the monolayer were harvested from the medium by centrifugation and were treated with trypsin, as indicated above, to control for the possible effects of the trypsin treatment. The cells were routinely tested and found to be free of *Mycoplasma* contamination.

Cell detachment studies. Cells were plated at a density of 1 × 10^4 cells/cm^2 in 75-cm^2 flasks with 10 ml of complete medium. After 48 hr, the medium was removed, and fresh drug-containing medium (20 ml) was added. VP-16 was resuspended in DMSO and mixed with the medium to a final DMSO concentration of 0.1%. CHX (Sigma Chemical Co.) was added from a 5 mM stock in PBS to a final concentration of 5 μM. Control cultures received an equal amount of vehicle in all experiments. At indicated times, the detached cells were harvested by centrifugation at 1000 × *g* for 5 min, and the original medium was returned to the flask. Cells were counted with the use of a hemocytometer after the addition of 0.2% Trypan blue (final concentration) in PBS. For determination of protein synthesis inhibition, cells were plated at a density of 7.5 × 10^4 cells/9.6 cm^2 into six-well plates (Falcon); 48 hr later, CHX was added at indicated concentrations, and protein synthesis was determined at indicated time points as previously described (25).

Morphological examination of cells. Attached and detached cells were harvested and centrifuged at 1000 × *g* for 5 min and resuspended in Puck's Saline A (GIBCO-BRL) containing 20 μg/ml Hoechst 33342 (Molecular Probes) for 15 min at room temperature. Nuclei were visualized using a Nikon Microphot-PX photomicroscope with an epifluorescence attachment. Electron microscopy was performed on attached cells *in situ* (50–100 cells were examined) and on sections of pelleted detached cells (50–100 cells were examined) as previously described (26).

DNA fragmentation. Attached cells either alone or in combination with detached cells from the same flask were harvested as above and centrifuged at 1000 × *g* for 5 min. The resulting cell pellet was lysed for 15 min in 100 μl (−)-*n*-octyl-β -glucopyranoside (0.75%; Boehringer Mannheim), 5 mM EDTA, and 5 mM Tris, pH 7.4, at 4°. After adjustment of the volume of the lysate to 4 ml, an aliquot was taken for determination of total DNA, and a second aliquot that had been centrifuged at 27,000 × *g* for 20 min was taken for determination of fragmented DNA in the supernatant (27). Both of these aliquots were reconstituted to 4 ml with 2 M NaCl, 5 mM EDTA, and 5 mM Tris, pH 7.4 (final concentrations), containing either 1.0 or 0.1 μg/ml Hoechst 33258 (Molecular Probes) to determine total and fragmented DNA, respectively, as previously described (28). DNA concentrations were determined from standard curves that routinely gave a correlation coefficient of ≥0.996 from 1.0 to 10 μg/ml for 1.0 μg/ml Hoechst 33258 and from 10 to 750 ng/ml for 0.1 μg/ml Hoechst 33258. Alternatively, cells were labeled with 0.1 μCi/ml [^{3}H-*methyl*]-thymidine (Amersham) for 48 hr. Cells were washed three times and incubated with fresh medium without radioisotope. After 2 hr, the medium was replaced, and drug was added. Attached cells were washed three times with PBS and harvested by trypsin treatment. Cells were then lysed with 0.5% Triton X-100 (molecular biology grade; Sigma), 5 mM EDTA, and 5 mM Tris, pH 7.4. Total and fragmented DNA were prepared as described above, and triplicate aliquots were counted with the use of a Beckman LS 1801 liquid scintillation counter.

Internucleosomal DNA cleavage. Cells were treated for 24, 48, and 72 hr with 1, 10, and 100 μM VP-16. Attached and detached cells were harvested as described above and analyzed for internucleosomal DNA cleavage as previously described (29).

QFIGE. Cells were harvested as in the above assay for DNA fragmentation; however, after centrifugation, cells were suspended to a final concentration of 2.5 × 10^4 cells/μl in a buffer containing 20 mM NaCl, 50 mM EDTA, and 10 mM Tris, pH 7.2, and equilibrated to 50°. An equal volume of 2% InCert (50°) agarose (FMC) was added, and plugs were cast (1 × 10^6 cells/plug) for QFIGE in disposable molds (Bio-Rad). After solidification at 4°, plugs were incubated at 50° overnight in 4.8 mM (0.2%) sodium deoxycholate, 1% sodium lauryl sarcosine, 100 mM EDTA, pH 8.0, and 1 mg/ml Proteinase K (Boehringer Mannheim) and then washed four times with 50 ml of 50 mM EDTA and 20 mM Tris, pH 8.0. For electrophoresis, plugs were uniformly cut so that 5 × 10^5 cells/lane were electrophoresed. Electrophoresis was performed with the use of an FIGE Mapper Electrophoresis System (Bio-Rad) in 1.5% Pulsed Field Certified Agarose (Bio-Rad) with a 0.5× Tris/borate/EDTA solution (45 mM Tris, 45 mM boric acid, 1 mM EDTA, pH 8.3) that was recirculated at 400 ml/min through a 6° water bath. During electrophoresis, the buffer was maintained at a constant temperature of 10 ± 0.5° in the electrophoresis chamber. An initial 12-min pulse of forward voltage at 150 V was applied to promote migration of the DNA from the plug into the gel. This initial pulse was followed by electrophoresis for 30 hr at 150 V using a 21% ramp from 0.9 to 30 sec in the forward direction and from 0.3 to 10 sec in the reverse direction at 10° (30). With a 21% ramp, the midpoint of the switch time ramp was reached after 21%

of the run time past. This nonlinearly shaped ramp was conducted in both the forward and reverse directions, always producing a 3:1 forward/reverse ratio, and allowed increased resolution of higher molecular weight DNA compared with a linear (50%) ramp. After electrophoresis, gels were stained with 1.0 μg/ml ethidium bromide for 1 hr. The gels were viewed with the use of a UV transilluminator and photographed. After photography, the gels were exposed to an additional 10 min of UV radiation on the transilluminator to allow sufficient nicking of DNA for alkali (0.4 N NaOH, 1.5 M NaCl, 24–36 hr) transfer of DNA to Zeta-Probe GT nylon membrane (Bio-Rad) through capillary action. Under these conditions, transfer of migrated DNA was complete, as indicated by the absence of ethidium bromide staining of agarose gels. Transfer of DNA that remained in the well was usually complete; however, the agarose near the wells was deformed due to surface tension of the agarose while casting the gel. This deformation sometimes resulted in incomplete transfer of nonmigrating DNA. The nylon membrane was neutralized by being soaked in 0.5 M Tris, pH 7.0, and then washed twice with 2× standard saline citrate (0.15 M NaCl, 0.015 M sodium citrate). After a 4–16-hr prehybridization (50% formamide, 5× standard saline/phosphate/EDTA [0.18 M NaCl, 10 mM NaH_2PO_4, 10 mM EDTA, pH 7.4] 2× Denhardt's reagent, 0.1% SDS), 25 ng of *alu*-I sequence probe (Oncogene Science) labeled with [α-^{32}P]dCTP (Amersham) was added. After overnight hybridization, the membranes were washed twice with 1× standard saline citrate and 0.1% SDS at 42°. The membranes were enveloped in plastic wrap and transferred to a phosphorimaging cassette for a 24–72-hr exposure. The phosphorimaging cassette was scanned with a model 425 PhosphorImager (Molecular Dynamics), and the resulting luminescence was quantified using ImageQuant (Molecular Dynamics). We tested this system on two separate occasions with a standard curve of [α-^{32}P]dCTP and found it to be linear $>10^5$ units, with each standard curve yielding correlation coefficients of ≥0.999. Molecular weight size standards were *Saccharomyces cerevisiae* chromosomes (225–2200 kbp, Bio-Rad) and λ phage digested with *Eco*RI and *Hin*dIII (8–48.5 kbp, GIBCO-BRL). Molecular weight standards were assigned to QFIGE gels based on migration distances of ethidium bromide-stained gels.

ISBE. Cells for ISBE were plated at a density of 1×10^4 cells/cm^2 in each well of a eight-well chamber slide (Nunc). After 48 hr, the medium was replaced with drug-containing medium and incubated for 2 hr at 37°. The cells were washed three times with PBS at 4° and subsequently fixed with 1% formaldehyde/PBS at 4° for 15 min, permeabilized by overnight incubation in 70% ethanol at −20°, and analyzed for DNA damage with 10 mM fluorescein-12-dUTP (Stratagene) and 200 units/ml terminal deoxynucleotidyl transferase, as previously described (31).

DNA Topoisomerase II/DNA covalent complex formation assay. DU-145 cells were plated as above and were labeled for 48 hr with 0.5 μCi/ml [^{3}H-*methyl*]thymidine (0.5 Ci/mM) and 0.1 μCi/ml [U-^{14}C]leucine (318 mCi/mmol) in complete medium. After 48 hr, cells were washed three times with complete medium, resuspended in fresh medium, and incubated for 1 hr at 37°. After 1 hr, the medium was replaced with fresh medium, and the cells were then grown in the presence or absence of melphalan (100 μM) or bleomycin (7 μM). After 24 hr, preapoptotic monolayer cells were washed three times with PBS and gently detached from the flask by scraping; detached apoptotic cells were discarded. After centrifugation (1000 × *g*), cell pellets were resuspended in a pH 7.4 buffer (buffer L; 110 mM NaCl, 5 mM KCl, 1 mM $MgCl_2$, 5 mM NaH_2PO_4, 25 mM HEPES, and 10 mM glucose) at a final concentration of 5×10^5 cell/ml. VP-16 (20 μM) or DMSO (0.4%) was added to 2 ml of cell suspension, and the cells were incubated for 30 min at 37°. After incubation, cells were pelleted by centrifugation (1000 × *g*) and lysed, cellular DNA was sheared by passage (four times) through a 22-gauge needle, and protein/DNA complexes were precipitated with SDS and KCl as previously described (32). DNA topoisomerase II/[^{3}H]/DNA complexes were quantified relative to ^{14}C-labeled protein by scintillation counting of KCl/SDS precipitates (32).

Statistical analysis. All statistical analyses were performed using InStat (GraphPad). Unless otherwise indicated, data were analyzed by analysis of variance followed by either Dunnett's or Student-Newman-Keuls multiple-comparison post hoc tests. Dunnett's post hoc tests were used when experimental groups were compared with a control group, whereas Student-Newman-Keuls post hoc tests were used when multiple comparisons between different experimental groups were required.

Results

VP-16 induced apoptosis in DU-145 cells. Initial clonogenic assays demonstrated that DU-145 cells were sensitive to the epipodophyllotoxin VP-16. Colony formation was inhibited with an IC_{50} of ~0.2 μM after a 7-day continuous VP-16 exposure (data not shown). Examination of cell survival after a 24-, 48-, or 72-hr VP-16 exposure revealed that DU-145 cells had a decrease in cell survival that was not only concentration but also time dependent (data not shown). Concomitant with a decrease in cell survival was an increase in the number of detached cells (Fig. 1A). After VP-16 exposure, cells asynchronously detached from the monolayer; the rate of detachment was greatest between 24 and 41 hr after

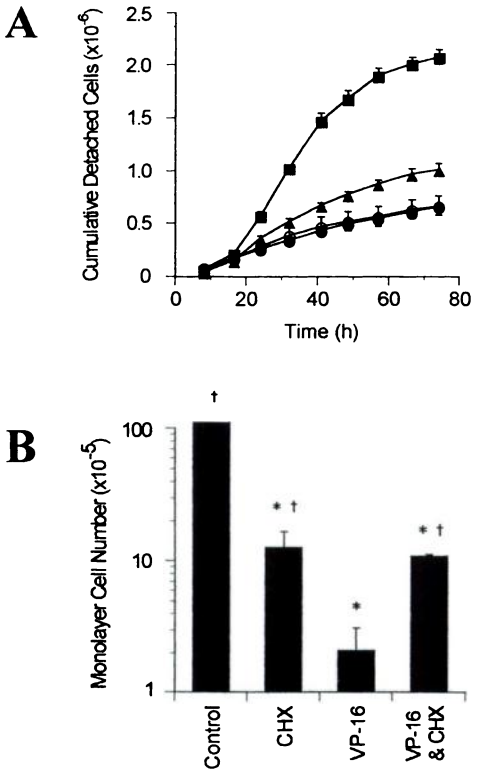

Fig. 1. Time-dependent VP-16-induced monolayer detachment and inhibition by cycloheximide. Exponentially growing DU-145 cells were treated with vehicle alone (●), 5 μM CHX (○), 30 μM VP-16 (■), or 30 μM VP-16 with 5 μM CHX (▲). A, Cell counts on detached cells were performed at 8–10-hr intervals over 74 hr. The number of cells detached in VP-16-treated cultures was significantly greater ($p < 0.05$) at all time points of ≥24 hr. Cultures treated with VP-16 and CHX were significantly different than VP-16-alone cultures at all time points of ≥24 hr; they also were significantly different from control cultures at all time points of ≥41 hr. B, Monolayer cell number in the flasks used for detachment studies after 74 hr of treatment. *, Significance versus control cultures at 74 hr. †, Significance versus 30 μM VP-16. Data represent cell counts from triplicate experiments; *error bars*, standard error.

VP-16 exposure, with ~60% of all cells detaching during this interval. Cotreatment with 5 μM CHX prevented much of the VP-16-induced detachment of cells from the monolayer, as demonstrated by a decrease in the number of detached cells (Fig. 1A). CHX treatment alone, however, was unable to lessen the basal rate of cell detachment, as CHX treatment did not suppress the number of detached cells versus control cultures. Furthermore, CHX only partially inhibited the detachment of cells from the monolayer as the CHX and VP-16 cotreatment resulted in significantly more detached cells than did CHX alone after 41 hr (Fig. 1A). Concomitant with the detachment of cells from the monolayer, VP-16 treatment caused a marked decrease in cells on the monolayer (Fig. 1B). Treatment with 5 μM CHX also caused a decrease in the number of cells on the monolayer, consistent with inhibition of protein synthesis. CHX treatment, however, partially blocked the VP-16-induced decrease in monolayer cell number to the level of CHX alone (Fig. 1B). The partial response of CHX may reflect incomplete blockage of protein synthesis; 5 μM CHX inhibited 85 ± 4% of protein synthesis at 0–8 hr, 78 ± 5% at 24 hr, and 72 ± 2% at 72 hr of continuous CHX exposure. Because treatment with 5 μM CHX alone caused inhibition of cell proliferation (Fig. 1B), we did not use higher concentrations of CHX to avoid toxicity during the time course.

The asynchronous detachment of these cells was further investigated with the use of time-lapse cinematography (data not shown). Before detachment from the monolayer, cells condensed, rounded, and developed numerous protuberances of the plasma membrane, until the cell ultimately detached from the monolayer. Further examination of attached and detached cells after staining with the DNA-binding fluorochrome Hoechst 33342 revealed DNA condensation and margination consistent with cell death via apoptosis in the VP-16-treated detached cells (Fig. 2C). Control DMSO-treated (Fig. 2A) and VP-16-treated (Fig. 2B) attached cells, however, had nuclear morphology that was characteristic of normal cells. Furthermore, attached control DMSO-treated cells or attached VP-16-treated cells exhibited normal nuclear chromatin structure when viewed with transmission electron microscopy (Fig. 2, D and E). In contrast, chromatin condensation and margination were readily observable in detached cell populations, as were numerous apoptotic bodies (Fig. 2F). From these data, we concluded that VP-16 induced apoptotic cell death in DU-145 cells.

Evaluation of DNA fragmentation. Exposure of DU-145 cells to VP-16 caused a concentration- and time-dependent increase in DNA fragmentation (Fig. 3A). VP-16 concentrations of ≥3 μM produced statistically significant ($p < 0.05$) increases in DNA fragmentation after 72 hr of continuous drug exposure. Higher concentrations of VP-16 (30–100 μM) induced statistically significant increases in DNA fragmentation by 24 hr. Interestingly, there was a concentration-dependent increase in DNA fragmentation in attached DU-

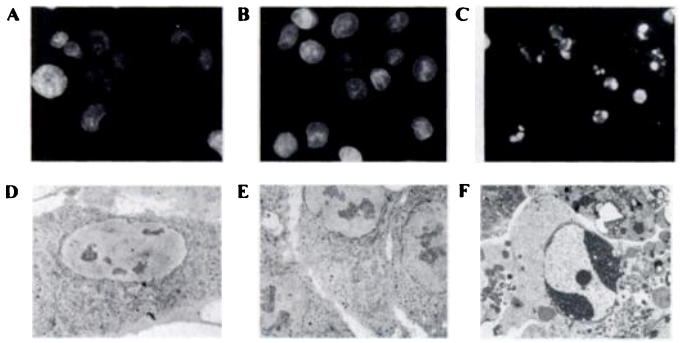

Fig. 2. Morphology of control and VP-16-treated DU-145 cells. Exponentially growing DU-145 cells were treated with 30 μM VP-16; after 24 hr, any detached cells were removed via centrifugation at 1000 × *g* for 5 min, the medium was replaced, and newly detached cells were collected over the next 4 hr. Therefore, all cells were incubated with 30 μM VP-16 or DMSO (*controls*) for a total of 28 hr. The newly detached cells were pelleted by centrifugation and either stained with Hoechst 33342 or fixed for electron microscopy. Attached cell populations were harvested by Trypsin treatment, pelleted by centrifugation, and stained with Hoechst 33342; alternatively, cells were fixed *in situ* for electron microscopy. A and D, Control attached cells. B and E, VP-16-treated attached cells. C and F, VP-16-treated detached cells. Final magnification: A–C, 600×; D and E, 2600×; and F, 4950×.

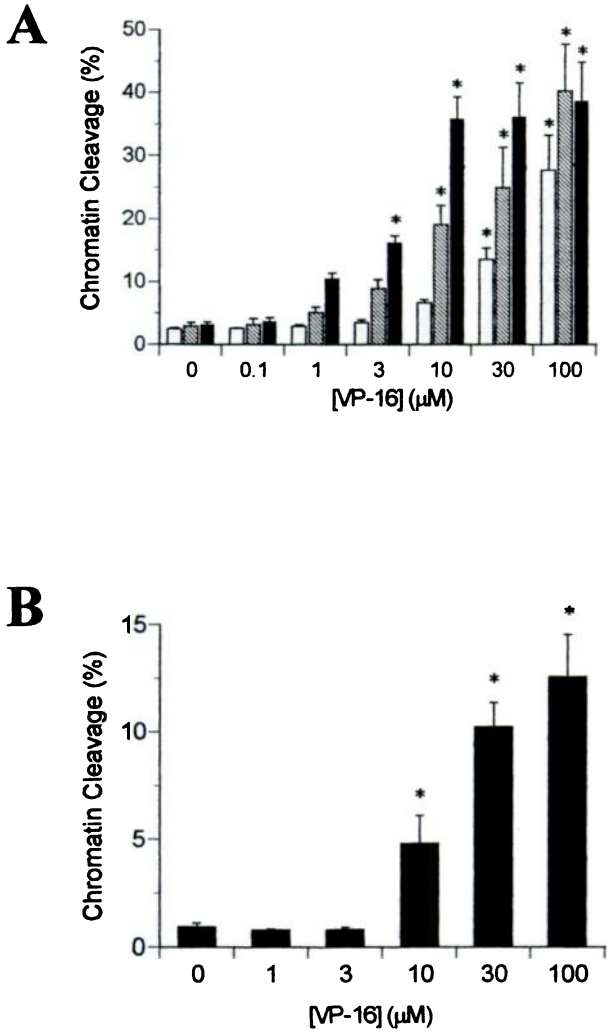

Fig. 3. Concentration- and time-dependent VP-16 induction of DNA fragmentation in DU-145 cells. Exponentially growing DU-145 cells were treated with VP-16; attached and detached cells were harvested and processed as described in Materials and Methods. Data represent mean DNA fragmentation (i.e., percentage of DNA not sedimented after a 27,000 × *g* centrifugation for 20 min) from five experiments (A) and three experiments (B); *error bars*, standard error. A, DNA fragmentation from attached and detached cells at 24 hr (*open bars*), 48 hr (*shaded bars*), and 72 hr (*solid bars*). B, DNA fragmentation from attached cells only 24 hr after VP-16 treatment. *, Significance versus DMSO ($p < 0.05$).

145 cells (Fig. 3B); these cell populations had normal morphology as determined with Hoechst 33342 staining (Fig. 2B) or transmission electron microscopy (Fig. 2E). Analysis of DNA from VP-16-treated DU-145 cells by conventional gel electrophoresis demonstrated an absence of internucleosomal DNA cleavage (data not shown).

Further examination of DNA fragmentation in attached VP-16-treated DU-145 cells with the use of QFIGE revealed production of discrete DNA fragments of ≥1 mbp, 450–600 kbp, and 30–50 kbp (Fig. 4A). Provocatively, each of these fragments was observed by QFIGE, in small quantities, in attached control cell populations (Fig. 4A), which may represent the basal apoptotic rate in control cell populations (Fig. 1A). Analysis of these attached cell populations revealed a concentration-dependent increase in higher order DNA fragmentation (Fig. 4B). ISBE and confocal microscopy also revealed a concentration-dependent increase in DNA strand breaks, with ~30% of the attached cells being positive 24 hr after exposure to 30 μM VP-16 (Fig. 5). In detached VP-16-treated cell populations, however, the ≥1-mbp and 450–600-kbp DNA fragments were virtually absent, and there was a tremendous accumulation of the 30–50-kbp DNA fragments (Fig. 4A). Trypsin/EDTA treatment of the detached cells did not affect the DNA fragmentation pattern (data not shown).

We investigated the possibility that these high molecular weight DNA fragments resulted from increased topoisomerase II/DNA interactions. First, kinetic analysis revealed that the increase in the ≥1-mbp and 450–600-kbp DNA fragments occurred simultaneously and was significant ($p < 0.05$) only after 10 hr of continuous exposure to 30 μM VP-16 (Fig. 6). In addition, the generation of the ≥1-mbp and 450–600-kbp DNA fragments was followed by a later (~2 hr) generation of the 30–50-kbp fragments. Second, the production of the ≥1-mbp, 450–600-kbp, and 30–50-kbp DNA fragments was also found to be partially inhibited (~50%) after a 24-hr continuous exposure to VP-16 by cotreatment with 5 μM CHX (Fig. 7). Further analysis of topoisomerase II levels by Western blot analysis using attached cell populations revealed no significant decrease in the amounts of topoisomerase II enzyme levels in 24-hr CHX-treated cells (data not shown). We also investigated the short term effects of CHX on inhibition of high molecular weight DNA fragmentation. With the use of ISBE, we observed an elevation of the mean fluorescence intensity in attached cells to 497 ± 15 arbitrary fluorescence units at 2 hr after the addition of 30 μM VP-16. This increase in fluorescence was totally abrogated when cells were simultaneously exposed to 30 μM VP-16 and 5 μM CHX, as the mean fluorescence intensity of attached cells was reduced to 373 ± 6, which was identical to the fluorescence intensity (377 ± 11) observed after exposure to only 5 μM CHX. Furthermore, CHX cotreatment also reduced the amount of DNA fragmentation observed with the use of QFIGE in the ≥1-mbp, 450–600-kbp, and the 30–50-kbp DNA fragments by 54 ± 1, 56 ± 3, and 36 ± 17, respectively. Finally, we investigated the ability of other agents to produce a similar profile of DNA fragmentation in these cells. In addition to VP-16,

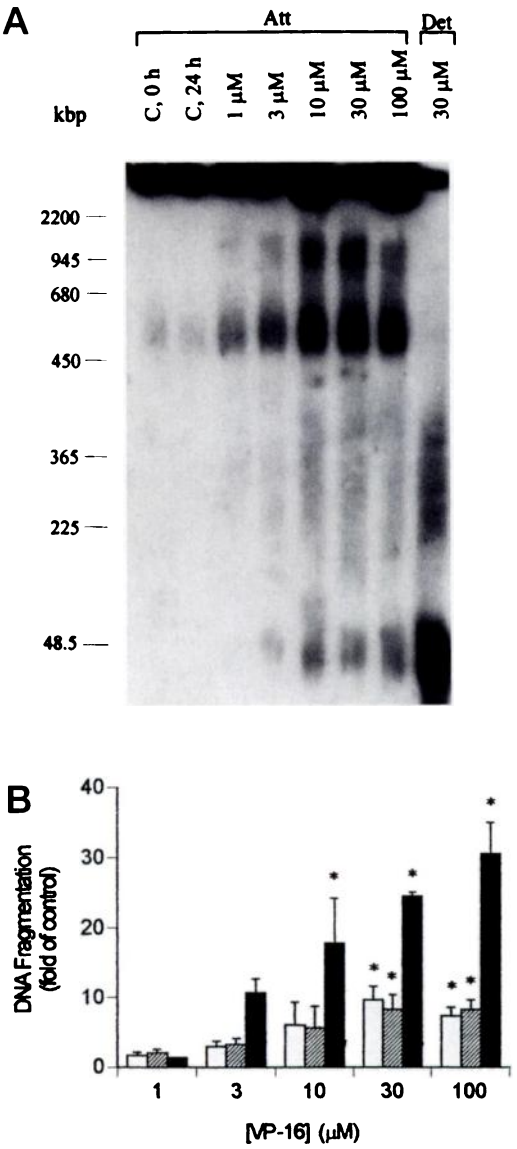

Fig. 4. QFIGE analysis of DNA fragmentation in DU-145 cells. A, Exponentially growing cells were treated with indicated concentrations of VP-16. After 24 hr, attached and detached cells were independently harvested, and agarose plugs were prepared as detailed in Materials and Methods. This figure is representative of three independent gels. B, Quantification of the DNA fragmentation observed from attached cells in A. *Open bars*, ≥1-mbp DNA fragments; *shaded bars*, 450–600-kbp DNA fragments; *solid bars*, 30–50-kbp DNA fragments. *Error bars*, standard error. *, Significance versus DMSO alone ($p < 0.05$).

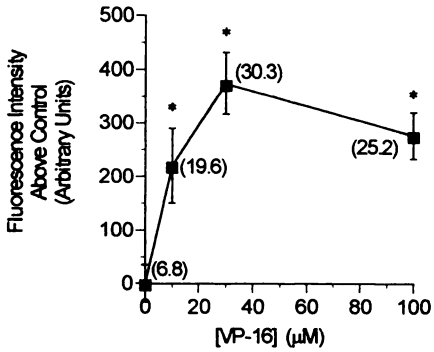

Fig. 5. DNA strand breaks in attached DU-145 cells 24 hr after treatment with VP-16. After 24-hr treatment, cells were processed for ISBE, and nuclear fluorescence intensity was measured. ■, Mean fluorescence intensity above DMSO alone. *Error bars*, standard error. *, Significance compared with DMSO alone ($p < 0.05$). *Values in parentheses*, percentage of cells with nuclear fluorescence intensity of ≥1000 arbitrary units.

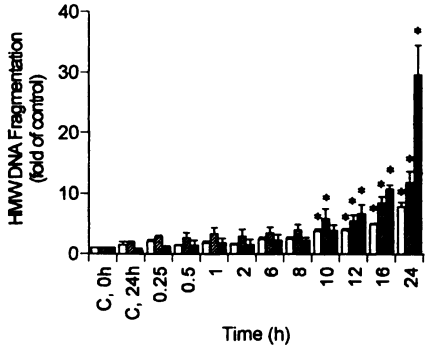

Fig. 6. Kinetic analysis of the production of ≥1-mbp, 450–600-kbp, and 30–50-kbp DNA fragments by QFIGE. Exponentially growing DU-145 cells were treated with 30 μM VP-16; at the indicated time points, attached cells were harvested and prepared in agarose plugs as described in Materials and Methods. Data were derived from quantification of three experiments. *, Significance compared with DMSO controls ($p < 0.05$). *Open bars* represent the ≥1-mbp DNA fragments. *Shaded bars*, 450–600-kbp DNA fragments; *solid bars*, 30–50-kbp DNA fragments.

melphalan (100 μM) and bleomycin (7 μM) not only produced a similar profile of high molecular weight DNA fragments but also produced ~5-fold more of each of the ≥1-mbp and 450–600-kbp DNA fragments compared with VP-16 (Fig. 8). The increased production of these fragments was not related to efficacy, as these agents were either as efficacious (melphalan) or less efficacious (bleomycin) than 30 μM VP-16 for induction of apoptotic morphology at 24 hr. Furthermore, all of these agents produced characteristic chromatin condensation and margination in detached cell populations, as shown in Fig. 2C, after Hoechst 33342 staining (data not shown). Also, to investigate whether melphalan and bleomycin were increasing topoisomerase II binding to DNA by a yet-undescribed pathway, we measured DNA/protein complexes in the absence or presence of 20 μM VP-16 after cells were incubated with melphalan or bleomycin for 24 hr. We observed no significant ($p < 0.05$) increase in DNA/protein binding in DMSO- or VP-16-treated cells regardless of whether these cells had been previously treated with melphalan or bleomycin (data not shown). Finally, there was no significant ($p < 0.05$) difference in topoisomerase II protein levels as assessed with Western blot analysis in attached (preapoptotic) melphalan- or bleomycin-treated cells (data not shown).

Discussion

The role of DNA fragmentation in apoptosis is highly debated. Internucleosomal DNA fragmentation, once considered the *sine qua non* of apoptosis, is actually a dispensable element of the apoptotic process in a variety of cell types (7–14). This finding antiquates the notion that internucleosomal DNA fragmentation is required for apoptosis. DNA fragmentation, however, remains a universal finding in nucleated cells during apoptosis; it has been suggested that DNA degradation during apoptosis may be a multistep process (7, 21, 33). Internucleosomal DNA cleavage may therefore represent a form of DNA fragmentation that is unnecessary, yet prevalent in many cell types undergoing apoptosis.

Results from several cell types reveal DNA fragments of ~5 mbp (6), >1 mbp (21), 700–800 kbp (19, 20), >600 kbp

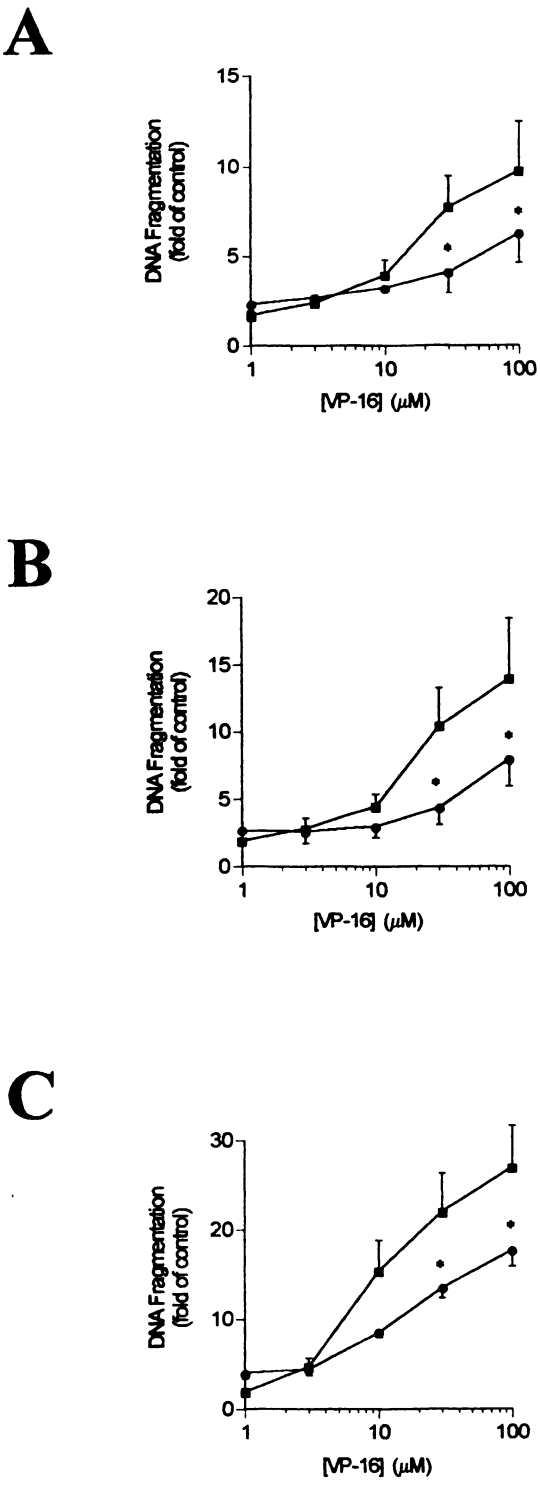

Fig. 7. Quantitative effect of cycloheximide on the VP-16-induced formation ≥1-mbp, 450–600-kbp, and 30–50-kbp DNA fragments as determined by QFIGE. The amount of fragmented DNA from QFIGE was determined as described in Materials and Methods. Data were obtained from quantification of the three independent experiments. A, ≥1-mbp DNA fragment. B, 450–600-kbp DNA fragment. C, 30–50-kbp DNA fragment. ■, Treatment with VP-16 alone. ●, Cotreatment with VP-16 and 5 μM. *, Significant reduction in DNA fragmentation compared with treatment with VP-16 alone ($p < 0.05$, paired Student's *t* test).

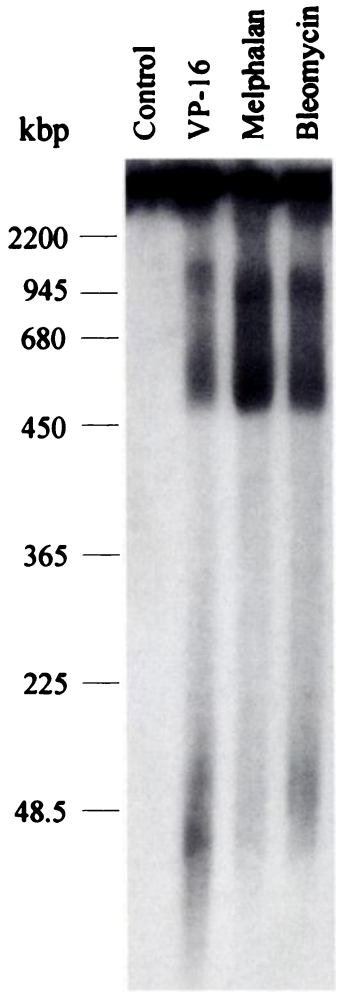

Fig. 8. Effect of melphalan and bleomycin on generation of high molecular weight DNA fragments. Exponentially growing cells were treated with 100 μM melphalan or 7 μM bleomycin. After 24 hr, cells were washed three times with PBS, attached cells were harvested, and agarose plugs were prepared as detailed in Materials and Methods. This figure is representative of three independent gels.

(23), ≥460 kbp (33), 200–300 kbp (7, 18–21, 33), 30–50 kbp (7, 18–21, 33), and 180 bp (and multiples thereof) occurring in apoptosis. Taken together with our results, these findings indicate that DNA fragmentation during apoptosis can be tentatively classified into four groups: class I, internucleosomal (180 bp) fragments, which does not occur in DU-145 cells; class II, 30–50-kbp DNA fragments; class III, 200–300-kbp DNA fragments; and class IV, >400-kbp DNA fragments. Furthermore, diversity of higher ordered DNA fragmentation may occur in different cell types, perhaps mediated by activation of different endonucleases. Nevertheless, some cell types have the capacity to produce fragments of multiple classes; for example, teniposide-treated murine lymphocytes produce DNA fragments of 700, 300, and 50 kbp and undergo internucleosomal DNA cleavage (20). The lack of class I DNA fragments in DU-145 cells, we believe, make them an attractive and useful model.

The observed differences in sizes of high molecular weight DNA fragments among various cell lines may represent differences in the endonucleases in these diverse cell types. Surprisingly, the enzymes responsible for DNA degradation during apoptosis are not known. Putative enzymes that produce internucleosomal (class I) fragments include a Ca^{2+}/Mg^{2+}-dependent endonuclease (34, 35), DNase I (36), DNase II (37), and NUC-18 (38). An Mg^{2+}-dependent/Ca^{2+}-independent endonuclease has been identified in rat thymocytes that may be responsible for some higher order chromatin cleavage (33).

Investigation of higher order DNA fragmentation in DU-145 human prostatic tumor cells revealed the production of discrete and quantifiable DNA fragments of ≥1 mbp, 450–600 kbp, and 30–50 kbp in the absence of internucleosomal DNA fragmentation. In prior studies, the presence of the >1-mbp, 700–800-kbp, and >600-kbp DNA fragments have been attributed to inhibition of the cleavable/religation reaction catalyzed by topoisomerase II (20, 21, 23). Supporting this idea is the loss of these large fragments if the topoisomerase-interactive drug teniposide is removed by washing (20, 21). The decline of the >1-mbp and 700–800-kbp fragments after drug removal in those particular studies was ascribed to the resealing of the topoisomerase II-cleavable complexes. In the present study, however, we observed DNA fragments of similar sizes (≥1 mbp and 450–600 kbp) that persisted after the removal of VP-16 by washing with PBS. Also, several results of the present study provide compelling evidence that these higher order DNA fragments in DU-145 cells are not generated as a result of increased topoisomerase II/DNA interactions during the induction of apoptosis but rather are likely to be generated by endonuclease activation. First, the increased generation of these class II and IV DNA fragments correlated temporally with induction of apoptosis and were not observed soon after VP-16 addition, as might be predicted if these DNA fragments were a result of VP-16-mediated stabilization of the DNA/topoisomerase II complex (Figs. 1 and 6). Second, formation of the high molecular weight DNA fragments was reduced at both 2 and 24 hr after VP-16 treatment by CHX coincubation, thereby demonstrating the essential role of protein synthesis. Third, the ≥1-mbp and 450–600-kbp DNA fragments were found after treatment with several pharmacological agents (i.e., melphalan and bleomycin) that are not thought to alter topoisomerase II activity (Fig. 8). Furthermore, the increased formation of the ≥1-mbp and 450–600-kbp DNA fragments in melphalan- and bleomycin-treated cells was not associated with increased topoisomerase II/DNA interactions (data not shown). Therefore, these results suggest a second interpretation of the aforementioned studies (20, 21), i.e., the loss of impetus for generation of the >1-mbp and 700–800-kbp fragments with the coordinated degradation of the >1-mbp and 700–800-kbp DNA fragments to 30–50-kbp DNA fragments.

In addition, it has recently been reported that a >600-kbp DNA fragment was produced soon (2 hr) after treatment of the human T lymphoblastoid cell line MOLT-4 with VP-16 (23). The abundance of this fragment was rapidly (≤5 min) reduced by washing with drug-free medium, a finding consistent with the reversible nature of topoisomerase II/DNA interactions. The generation of high molecular weight DNA fragmentation in the MOLT-4 cell line is in opposition to our findings in DU-145 cells with respect to several important elements. We observed the production of these high molecular weight DNA fragments only after prolonged incubation with VP-16 in DU-145 cells (Fig. 6) compared with relatively rapid (2 hr) formation of the >600-kbp DNA fragment in MOLT-4 cells. Furthermore, we detected a similar pattern of

DNA fragmentation in DU-145 cells when treated with agents (i.e., melphalan and bleomycin) that are not thought to act through topoisomerase II and were found not to either increase basal DNA/protein complex formation or alter the ability of VP-16 to induce covalent complex formation. MOLT-4 cells grow in suspension rather than as a monolayer, as do the DU-145 cells and most other non-leukemic/lymphoid cell types. Matrix attachment can affect the apoptotic process (31); thus, further investigation of these differences is warranted. In particular, it would be interesting to induce apoptosis in MOLT-4 cells using a variety of agents, including melphalan and bleomycin, to gain further insight into the apparent topoisomerase II-mediated generation of the >600-kbp DNA fragment in this suspension cell type.

In summary, we found that apoptosis induced by VP-16, melphalan, and bleomycin in DU-145 cells is characterized by the cleavage of DNA into ≥1-mbp and 450–600-kbp fragments before cell detachment or morphological changes in chromatin structure. Quantification of discrete high molecular weight DNA fragments with the use of QFIGE illustrates the usefulness of this new tool for investigating early events (i.e., before morphological changes) in apoptosis. Accrual of 30–50-kbp DNA fragments in detached cell populations, however, is coincident with chromatin condensation, and from kinetic analysis we conclude that the ≥1-mbp and 450–600-kbp DNA fragments are precursors to these fragments. Furthermore, the lack of apoptotic morphology in attached cells and the lack of further DNA degradation onto oligonucleosomal-sized DNA fragments in this cell line designate the 30–50-kbp DNA fragments as possible mediators of the changes in nuclear morphology, which define apoptosis. Finally, in androgen-independent human prostatic carcinoma cells, DNA fragmentation is the earliest identified marker of apoptosis. The presence of high molecular weight DNA fragmentation in attached cells may demarcate a preapoptotic cell population and may also represent a concomitant event in drug-induced apoptosis.

Acknowledgments

We thank Dr. Caroline Dive for assistance in initial examination of DU-145 cells for apoptosis. The thoughts, comments, and technical assistance of Dr. Simon C. Watkins, Dr. John A. Hickman, Dr. Mary K. Ritke, William P. Allan, and Catherine E. Settineri are also appreciated.

References

1. Shi, Y. F., J. M. Glynn, L. J. Guilbert, T. G. Cotter, R. P. Bissonnette, and D. R. Green. Role of c-myc in activation-induced apoptotic cell death in T cell hybridomas. *Science (Washington D. C.)* **257:**212–214 (1992).
2. Wyllie, A. H. Apoptosis (The 1992 Frank Rose Memorial Lecture). *Br. J. Cancer* **67:**205–208 (1993).
3. Eaton, C. L., P. Davies, M. Harper, T. France, N. Rushmere, and K. Griffiths. Steroids and the prostate. *J. Steroid Biochem. Mol. Biol.* **40:**175–183 (1991).
4. Kerr, J. F. R., A. H. Wyllie, and A. R. Currie. Apoptosis: a basic biological phenomenon with wide-ranging implications in tissue kinetics. *Br. J. Cancer.* **26:**239–257 (1972).
5. Wyllie, A. H., R. G. Morris, A. C. Smith, and D. Dunlop. Chromatin cleavage in apoptosis: association with condensed chromatin morphology and dependence on macromolecular synthesis. *J. Pathol.* **142:**67–77 (1984).
6. Canman, C. E., H. Y. Tang, D. P. Normolle, T. S. Lawrence, and J. Maybaum. Variations in patterns of DNA damage induced in human colorectal tumor cells by 5-fluorodeoxyuridine: implications for mechanisms of resistance and cytotoxicity. *Proc. Natl. Acad. Sci. USA* **89:**10474–10478 (1992).
7. Oberhammer, F., J. W. Wilson, C. Dive, I. D. Morris, J. A. Hickman, A. E. Wakeling, P. R. Walker, and M. Sikorska. Apoptotic death in epithelial cells: cleavage of DNA to 300 and/or 50 kb fragments prior to or in the absence of internucleosomal fragmentation. *EMBO J.* **12:**3679–3684 (1993).
8. Oberhammer, F., W. Bursch, R. Tiefenbacher, G. Fröschl, M. Pavelka, T. Purchio, and R. Schulte-Hermann. Apoptosis is induced by transforming growth factor-β1 within 5 hours in regressing liver without significant fragmentation of the DNA. *Hepatology* **18:**1238–1246 (1993).
9. Barbieri, D., L. Troiano, E. Grassilli, C. Agnesini, E. A. Cristofalo, D. Monti, M. Capri, A. Cossarizza, and C. Franceschi. Inhibition of apoptosis by zinc: a reappraisal. *Biochem. Biophys. Res. Commun.* **187:**1256–1261 (1992).
10. Tomei, L. D., J. P. Shapiro, and F. O. Cope. Apoptosis in C3H/10T1/2 mouse embryonic cells: evidence for internucleosomal DNA modification in the absence of double-strand cleavage. *Proc. Natl. Acad. Sci. USA* **90:**853–857 (1993).
11. Falcieri, E., A. M. Martelli, R. Bareggi, A. Cataldi, and L. Cocco. The protein kinase inhibitor staurosporine induces morphological changes typical of apoptosis in MOLT-4 cells without concomitant DNA fragmentation. *Biochem. Biophys. Res. Commun.* **193:**19–25 (1993).
12. Ormerod, M. G., C. F. O'Neill, D. Robertson, and K. R. Harrap. Cisplatin induces apoptosis in a human ovarian cell line without concomitant internucleosomal degradation of DNA. *Exp. Cell Res.* **211:**231–237 (1994).
13. Ucker, D. S., P. S. Obermiller, W. Eckhart, J. R. Apgar, N. A. Berger, and J. Meyers. Genome digestion is a dispensable consequence of physiologic cell death mediated by cytotoxic T lymphocytes. *Mol. Cell. Biol.* **12:**3060–3069 (1992).
14. Cohen, G. M., X.-M. Sun, R. T. Snowden, D. Dinsdale, and D. N. Skilleter. Key morphological features of apoptosis may occur in the absence of internucleosomal DNA fragmentation. *Biochem. J.* **286:**331–334 (1992).
15. Schulze-Osthoff, K., H. Walczak, W. Droge, and P. H. Krammer. Cell nucleus and DNA fragmentation are not required for apoptosis. *J. Cell Biol.* **127:**15–20 (1994).
16. Jacobson, M. D., J. F. Burne, and M. C. Raff. Programmed cell death and Bcl-2 protection in the absence of a nucleus. *EMBO J.* **13:**1899–1910 (1994).
17. Ormerod, M. G., C. F. O'Neill, D. Robertson, and K. R. Harrap. Cisplatin induces apoptosis in a human ovarian carcinoma cell line without concomitant internucleosomal degradation of DNA. *Exp. Cell Res.* **211:**231–237 (1994).
18. Brown, D. G., X.-M. Sun, and G. M. Cohen. Dexamethasone-induced apoptosis involves cleavage of DNA to large fragments prior to internucleosomal fragmentation. *J. Biol. Chem.* **268:**3037–3039 (1993).
19. Walker, P. R., C. Smith, T. Youdale, J. Leblanc, J. F. Whitfield, and M. Sikorska. Topoisomerase II-reactive chemotherapeutic drugs induce apoptosis in thymocytes. *Cancer Res.* **51:**1078–1085 (1991).
20. Roy, C., D. L. Brown, J. E. Little, B. K. Valentine, P. R. Walker, M. Sikorska, J. Leblanc, and N. Chaly. The topoisomerase II inhibitor teniposide (VM-26) induces apoptosis in unstimulated mature murine lymphocytes. *Exp. Cell Res.* **200:**416–424 (1992).
21. Walker, P. R., L. Kokileva, J. LeBlanc, and M. Sikorska. Detection of the initial stages of DNA fragmentation in apoptosis. *Biotechniques* **15:**1032–1040 (1993).
22. Corbett, A. H., and N. Osheroff. When good enzymes go bad: conversion of topoisomerase II to a cellular toxin by antineoplastic drugs. *Chem. Res. Toxicol.* **6:**585–597 (1993).
23. Beere, H. M., C. M. Chresta, A. Alejo-Herberg, A. Skladanowski, C. Dive, and J. A. Hickman. Investigation of the mechanism of higher order chromatin fragmentation observed in drug-induced apoptosis. *Mol. Pharmacol.* **47:**986–996 (1995).
24. Stone, K. R., D. D. Mickey, H. Wunderli, G. H. Mickey, and D. F. Paulson. Isolation of a human prostate carcinoma cell line (DU 145). *Int. J. Cancer* **21:**274–281 (1978).
25. Schnitzlein, W. M., M. K. O'Banion, M. K. Poirot, and M. E. Reichmann. Effect of intracellular vesicular stomatitis virus mRNA concentration on the inhibition of host cell protein synthesis. *J. Virol.* **45:**206–214 (1983).
26. Watkins, S. C., and M. J. Cullen. A quantitative study of myonuclear and satellite cell nuclear size in Duchenne's muscular dystrophy, polymyositis and normal human skeletal muscle. *Anat. Rec.* **222:**6–11 (1988).
27. Wyllie, A. H., and R. G. Morris. Hormone-induced cell death. Purification and properties of thymocytes undergoing apoptosis after glucocorticoid treatment. *Am. J. Pathol.* **109:**78–87 (1982).
28. Labarca, C., and K. Paigen. A simple, rapid, and sensitive DNA assay procedure. *Anal. Biochem.* **102:**344–352 (1980).
29. Kyprianou, N., and J. T. Isaacs. 'Thymineless' death in androgen-independent prostatic cancer cells. *Biochem. Biophys. Res. Commun.* **165:**73–81 (1989).
30. Denko, N., A. Giaccia, B. Peters, and T. D. Stamato. An asymmetric field inversion gel electrophoresis method for the separation of large DNA molecules. *Anal. Biochem.* **178:**172–176 (1989).
31. Hoyt, D. G., R. J. Mannix, J. M. Rusnak, B. R. Pitt, and J. S. Lazo. Collagen is a survival factor against LPS-induced apoptosis in cultured sheep pulmonary artery endothelial cells. *Am. J. Physiol.* **269:**L171–L177 (1995).

32. Zwelling, L. A., M. Hinds, D. Chan, J. Mayes, K. L. Sie, E. Parker, L. Silberman, A. Radcliffe, M. Beran, and M. Blick. Characterization of an amsacrine-resistant line of human leukemia cells: evidence for a drug-resistant form of topoisomerase II. *J. Biol. Chem.* **264:**16411–16420 (1989).
33. Sun, X. M., and G. M. Cohen. Mg^{2+}-dependent cleavage of DNA into kilobase pair fragments is responsible for the initial degradation of DNA in apoptosis. *J. Biol. Chem.* **269:**14857–14860 (1994).
34. Cohen, J. J., and R. C. Duke. Glucocorticoid activation of a calcium-dependent endonuclease in thymocyte nuclei leads to cell death. *J. Immunol.* **132:**38–42 (1984).
35. Arends, M. J., R. G. Morris, and A. H. Wyllie. Apoptosis: the role of the endonuclease. *Am. J. Pathol.* **136:**593–608 (1990).
36. Peitsch, M. C., B. Polzar, H. Stephan, T. Crompton, H. R. MacDonald, H. G. Mannherz, and T. Jürg. Characterization of the endogenous deoxyribonuclease involved in nuclear DNA degradation during apoptosis (programmed cell death). *EMBO J.* **12:**371–377 (1993).
37. Barry, M. A., and A. Eastman. Identification of deoxyribonuclease II as an endonuclease involved in apoptosis. *Arch. Biochem. Biophys.* **300:**440–450 (1993).
38. Gaido, M. L., and J. A. Cidlowski. Identification, purification, and characterization of a calcium-dependent endonuclease (NUC18) from apoptotic rat thymocytes: NUC18 is not histone H2B. *J. Biol. Chem.* **266:**18580–18585 (1991).

Send reprint requests to: Dr. John S. Lazo, Department of Pharmacology, E1340 Biomedical Science Tower, University of Pittsburgh School of Medicine, Pittsburgh, PA 15261.